Technische Universität Chemnitz

Sonderforschungsbereich 393

Numerische Simulation auf massiv parallelen Rechnern

Thomas Apel · Sergei Grosman

Peter K. Jimack · Arnd Meyer

A New Methodology for Anisotropic Mesh Refinement Based Upon Error Gradients

Preprint SFB393/01-11

Abstract We introduce a new strategy for controlling the use of anisotropic mesh refinement based upon the gradients of an *a posteriori* approximation of the error in a computed finite element solution. The efficiency of this strategy is demonstrated using a simple anisotropic mesh adaption algorithm and the quality of a number of potential *a posteriori* error estimates is considered.

Key Words Anisotropic refinement, *A posteriori* error estimation, Finite element method.

AMS(MOS) subject classification 65N50, 65N30.

Preprint-Reihe des Chemnitzer SFB 393

SFB393/01-11 **March 2001**

Contents

Author's addresses:

Thomas Apel, Sergei Grosman, Arnd Meyer
TU Chemnitz
Fakultät für Mathematik
D-09107 Chemnitz, Germany

Peter K. Jimack
Computational PDE Unit, School of Computing
University of Leeds
Leeds LS2 9JT, UK

1 Introduction

The use of anisotropic mesh refinement in the adaptive finite element solution of partial differential equations (PDEs) with highly anisotropic solutions is widely recognised as having significant potential for improving the efficiency of the solution process, e.g. [3, 5, 10, 18, 22, 28]. Numerous schemes for driving anisotropic mesh adaptivity have been considered in both the engineering, [3, 9, 10, 22, 27, 28], and the numerical analysis literature, [12, 25, 26]. Typically, such schemes fall into two broad categories: based either on *a priori* knowledge of the nature of the solution (e.g. [6, 20]) or on more *ad hoc* indicators which tend to use features of the equation or the numerical solution to drive the refinement (e.g. [8, 14, 16, 24]). In this communication we propose an alternative technique for driving anisotropic mesh refinement based upon *a posteriori* error estimation.

Throughout this paper we focus on a linear, second order, reaction-diffusion test problem

$$-\Delta u + \kappa^2 u = f; \qquad u \in \Omega = (0,1) \times (0,1), \tag{1}$$

with Dirichlet boundary conditions on $\partial\Omega$. Note that when $f = 0$ equation (1) is satisfied by

$$u = e^{-\kappa x} + e^{-\kappa y} \tag{2}$$

which features highly anisotropic boundary layers when $\kappa \gg 1$. In order to assess the quality of our proposed mechanism for driving the mesh adaptivity, described in Sections 2 and 3 we only use a very simple mesh refinement algorithm in this work. This allows us to separate out the issue that we are concerned with here, of how to drive the anisotropic refinement (i.e. provide the information needed to decide where an existing mesh needs to be refined and in which directions) in a robust manner, from the (equally important) issue of how to execute the refinement (i.e. the precise mechanisms and data structures used to implement the refinement: see, for example, [11, 17, 23] for work in this area). The paper concludes with a discussion of a number of important implementation issues and an assessment of the potential of our new approach.

2 An adaptive strategy

The natural norm in which to measure the error of a numerical approximation to the solution of (1) is the energy norm given by

$$|||v|||^2 = \|\frac{\partial v}{\partial x}\|^2 + \|\frac{\partial v}{\partial y}\|^2 + \kappa^2 \|v\|^2 \,, \tag{3}$$

where $\|\cdot\|$ represents the usual L^2 norm over Ω. When a set of finite element solutions is obtained using a nested sequence of progressively larger trial spaces (based upon conventional, isotropic, h-refinement for example), the final term on the right-hand side of (3) will tend to zero faster than the other two. It may be the case however that, although tending to zero at the same asymptotic rate, the ratio between these two dominant terms

is far from one. Our proposal is to drive an anisotropic mesh refinement algorithm based upon the target of equilibrating these two terms, on each element, before reducing them at the same rate using conventional h-refinement. Although the asymptotic convergence rate will not be improved by such a strategy, we expect to see a significant computational gain.

In order to demonstrate the effectiveness of the proposed strategy we begin by considering the exact error to equation (1),

$$e^h = u - u^h \ , \tag{4}$$

where u is given by (2) and u^h is the Galerkin finite element solution to (1) (with $f = 0$), subject to exact Dirichlet boundary conditions, on a given mesh. Moreover, we also consider only a very straightforward anisotropic refinement algorithm based upon the refinement of rectangles in one of the three ways illustrated in Figure 1. This is a simplification of the algorithm suggested in [23].

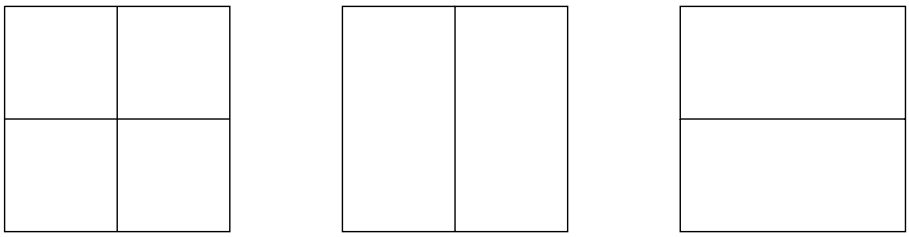

Figure 1: The three types of refinement allowed: regular (left), anisotropic in x (middle) and anisotropic in y (right).

When an error on a particular rectangle exceeds some tolerance (typically 20% of the maximum error over all rectangles) it is refined. If the $\kappa^2\|e^h\|$ component of the error is dominant on a rectangle (i.e. $\kappa^2\|e^h\|^2 > C|||e^h|||^2$, where C is typically chosen to equal $\frac{1}{2}$), or if

$$\|\frac{\partial e^h}{\partial x}\| / \|\frac{\partial e^h}{\partial y}\| \in [\frac{1}{2}, 2] \ , \tag{5}$$

then regular refinement takes place on that rectangle. Otherwise, anisotropic refinement takes place: refining in x when $\|\frac{\partial e^h}{\partial x}\|$ dominates and in y when $\|\frac{\partial e^h}{\partial y}\|$ dominates. Rectangles are also refined when any edges contain two or more "hanging nodes" (due to successive refinement of a neighbour) so as to prevent excessively large changes in h_x or h_y (the mesh sizes in the x and y directions respectively).

Figure 2 illustrates graphs of the error against the number of finite element unknowns when equation (1) is solved, with $\kappa = 10^3$, using the above refinement strategy. In the first (left) case $f = 0$ and the exact solution is (2), whilst in the second (right) case $f \neq 0$ and the Dirichlet boundary conditions are chosen so as to permit the exact solution

$$u = e^{-\kappa x} + e^{-\kappa y} + x^2 + \cos(10y) \ . \tag{6}$$

The main difference between these two cases is that u is essentially zero away from the boundary in the former but is a smooth non-zero function away from the boundary in the latter. The three graphs plotted in each case are all obtained using the same initial isotropic mesh (where each element has an aspect ratio of 1) and correspond to artificially imposing a maximum element aspect ratio after refinement of 1 (i.e. only regular refinement allowed), 16 and 256 respectively. For the purposes of this work we define the aspect ratio (AR) of a rectangular element to be $\max(h_x/h_y, h_y/h_x)$. Furthermore, all finite element calculations are performed using piecewise linear elements obtained by dividing each rectangle into two triangles (with exceptional divisions into three or four triangles when hanging nodes are present). A discussion of the use of even larger aspect ratios is postponed until Section 4.

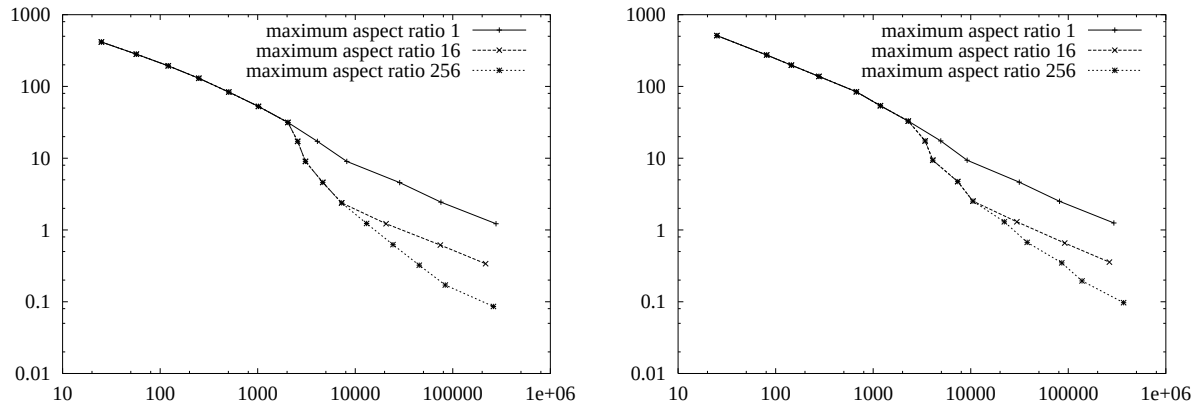

Figure 2: Graphs of the error as a function of the number of unknowns for the two test problems (with $\kappa = 10^3$) with a maximum possible aspect ratio of 1 (upper), 16 (middle) and 256 (lower) in each case. For each calculation the adaptivity is based upon the energy norm of the (known) exact error, calculated using a seven point quadrature rule with degree of precision five.

The results shown in Figure 2 are typical of those obtained for all large values of κ and clearly show a significant advantage from the use of our anisotropic refinement strategy. Note that the asymptotic convergence rates are the same in all cases so the improvement is by a constant factor. Also note that in both examples our adaptive algorithm begins with uniform refinement to drive down the large initial L^2 error before the advantage of using anisotropic refinement is seen.

3 *A posteriori* error estimation

Whilst the numerical results exemplified by those presented in the previous section are extremely encouraging, it is clear that for the proposed methodology to be of any practical value a similar quality of results must also be achievable using *a posteriori* error estimates (as opposed to the exact error). Recently there has been a significant amount of research into the development and analysis of *a posteriori* error estimates that are effective on

highly anisotropic grids (see, for example, [13, 18, 19, 25]). Our requirement is even more demanding than this however, since we are restricted to consider only those techniques which yield local estimates of the error as a function: thus enabling us to compute each of the three L^2 norms that appear in (3) on each element.

For the purposes of this investigation we have selected a small number of well-known *a posteriori* error estimation algorithms and contrasted their use with that of the exact error as described in the previous section. The algorithms considered are shown in Table 1, with the first three (AB, AO and BW) all requiring the solution of a local error equation on each element. In contrast with this, the ZZ approach involves a direct approximation of the gradients of the error on each element and therefore provides no estimate of $\|e^h\|$. Since all of these error estimators are defined on triangles piecewise linear triangular finite elements have again been used, as described in the previous section.

Abbrv.	Reference	Comments
AB	Ainsworth & Babuška [1]	A generalisation of AO designed for large κ
AO	Ainsworth & Oden [2]	The equilibrated residual method
BW	Bank & Weiser [7]	We use the third algorithm from this paper
ZZ	Zienkiewicz & Zhu [29]	Provides approximations of $\|\frac{\partial e^h}{\partial x}\|$ and $\|\frac{\partial e^h}{\partial y}\|$ only

Table 1: Descriptions of the error estimators used in this paper.

In order to assess the suitability of these indicators for our purposes, we return to the calculations that led to the best results shown in Figure 2 (i.e. with a maximum aspect ratio of 256). Both of these calculations are repeated and after each finite element solve we not only compute the exact error function, e^h, but also each of the *a posteriori* estimates (η^h say) described above. Table 2 presents the results of these calculations in the form of effectivity ratios $|||\eta^h|||/|||e^h|||$. (Note however that for the ZZ error estimate we have no contribution from the L^2 part of the error.)

The results presented in Table 2 show that on very coarse meshes, where all elements have an aspect ratio of one, the AB and the BW estimates both appear to perform quite well, and as the meshes are refined uniformly the effectivity index gets closer to one in each case. However, when anisotropic refinement begins to occur the quality of these estimates tends to deteriorate as the maximum aspect ratio grows. This is clearly a potentially undesirable property for our approach. Similar behaviour is observed for the AO algorithm when anisotropic refinement occurs, although this is perhaps not surprising since this estimate yields the same approximation as AB when an element is sufficiently small. For the coarse initial meshes the AO estimate always overestimates the error.

The ZZ estimate is extremely poor on the very coarse meshes, which is due to the fact that it does not approximate the L^2 component of the energy norm of the error. Once this component has been driven down through regular refinement however the ZZ estimate performs well: consistently yielding an effectivity index of between about 0.6 and 0.7. Most significantly, this is the only one of the four estimates considered which does not appear to be adversely affected by the increasing aspect ratio.

Problem 1					Problem 2				
Vertices (AR)	AB	AO	BW	ZZ	Vertices (AR)	AB	AO	BW	ZZ
25 (1)	0.83	1.36	0.72	0.01	25 (1)	0.87	2.45	0.82	0.01
57 (1)	0.86	1.42	0.74	0.01	81 (1)	0.84	1.40	0.71	0.01
121 (1)	0.89	1.45	0.76	0.02	145 (1)	0.87	1.55	0.74	0.02
249 (1)	0.91	1.47	0.78	0.04	294 (1)	0.91	1.68	0.78	0.04
505 (1)	0.96	1.47	0.81	0.09	673 (1)	0.99	1.49	0.83	0.09
1017 (1)	1.04	1.36	0.86	0.18	1185 (1)	1.07	1.42	0.88	0.18
2041 (1)	1.11	1.19	0.93	0.36	2288 (1)	1.11	1.39	0.93	0.35
2567 (2)	1.20	1.21	1.03	0.56	3407 (2)	1.19	1.25	1.02	0.56
3086 (4)	1.40	1.41	1.08	0.66	4077 (4)	1.38	1.51	1.07	0.64
4643 (8)	1.63	1.63	1.15	0.72	7351 (8)	1.60	1.70	1.14	0.70
7256 (16)	1.84	1.84	1.20	0.70	10533 (16)	1.78	1.91	1.17	0.67
13074 (32)	2.16	2.16	1.36	0.65	22090 (32)	2.09	2.15	1.31	0.62
24352 (64)	2.69	2.69	1.62	0.62	37921 (64)	2.56	2.59	1.54	0.60
45380 (128)	3.44	3.44	2.20	0.61	85764 (128)	3.24	3.25	2.07	0.59
83515 (256)	4.41	4.41	3.41	0.60	138298 (256)	3.93	3.94	2.99	0.58
259578 (256)	3.66	3.66	3.25	0.59	368598 (256)	3.30	3.30	2.84	0.58

Table 2: The effectivity ratios of a number of error estimates when the adaptive algorithm (based upon the elementwise energy norm of the exact error) is applied to the two test problems with a maximum permitted aspect ratio of 256. The first column for each problem gives the total number of vertices in each mesh along with the maximum aspect ratio of any rectangle in that mesh.

Having assessed the effectiveness of our selected error estimators on sequences of meshes determined from the exact error, we now contrast these meshes with those obtained when the adaptivity is driven by the estimated errors. Results for the same two examples, with the same maximum aspect ratio of 256, are presented in Figure 3. The graphs shown are of the exact error in each case but do not include the graph for the AO estimate. This is because it turns out that, despite providing different numerical values to AB on the coarse initial grids, this estimate leads to very similar sequences of grids to those obtained using AB in both examples (the graphs of error against unknowns are almost indistinguishable).

The graphs shown in Figure 3 are again typical of those obtained for other large values of κ. In both examples we see that the AB error estimate proves to be a better driver of the adaptivity than BW, despite there being little to choose between them from the results presented in Table 2. In particular, once the aspect ratio becomes significantly greater than one, the AB estimate appears to provide the better indication of the relative sizes of $\|\frac{\partial e^h}{\partial x}\|$ and $\|\frac{\partial e^h}{\partial y}\|$ on each element.

The ZZ estimate also leads to interesting behaviour in these two tests. In each case it begins anisotropic refinement much sooner than any of the other estimates permit since it

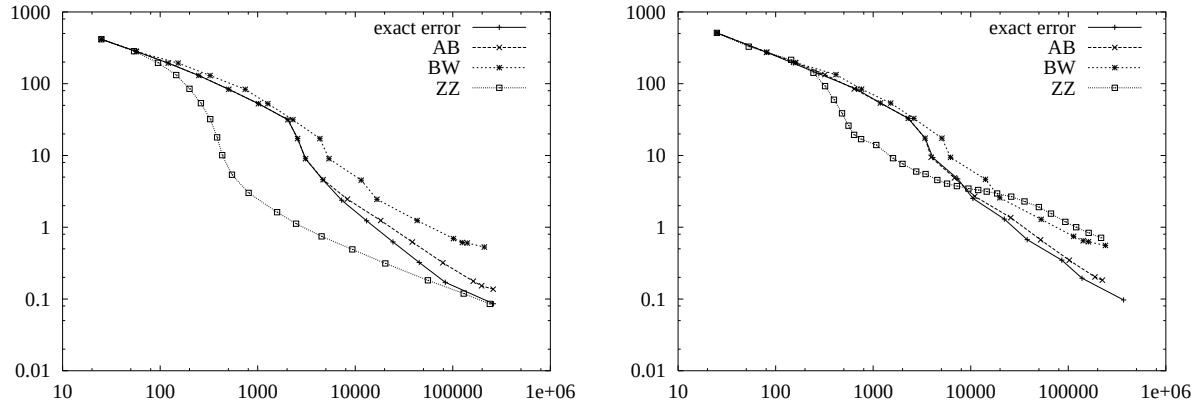

Figure 3: Graphs of the error as a function of the number of unknowns for the two test problems (with $\kappa = 10^3$ and a maximum aspect ratio 256). Each problem is solved four times: the adaptivity being driven by the exact error and the error estimates AB, BW and ZZ.

has no approximation of the L^2 component of the error. Hence the condition

$$\kappa^2 \|e^h\|^2 \leq C|||e^h|||^2 \tag{7}$$

is always satisfied. In the first example this proves to be advantageous (thus demonstrating that our choice of $C = \frac{1}{2}$ in (7) is over-cautious in this case), leading to the maximum aspect ratio of 256 being reached far sooner than when the exact error is used. Since the ZZ estimate is apparently unaffected by these large aspect ratios it continues to do well and ultimately leads to meshes of almost identical quality to those obtained using the exact error to drive the adaptivity. In the second example however, where the solution is a non-zero function away from the boundary, the ZZ estimate performs less well. Again it leads to anisotropic refinement in the boundary layer sooner than the other estimates but, since the L^2 component of the error in the interior has not been eliminated at this stage, the adaptive algorithm runs into difficulties later on.

Overall therefore, we see that, of the error estimates considered, the AB estimate would appear to be the most appropriate to use in the practical situation where the exact error is unavailable. Nevertheless, it is unlikely that this is an optimal choice and, as described in the next section, provides some implementation difficulties when the aspect ratio becomes extremely large.

4 Implementation issues

The results presented in the preceding sections are a small selection from a much larger number of computations, performed with a variety of different parameter choices. In this section we provide a brief overview of some of these parameters, such as the maximum aspect ratio, the interval in (5) and the constant C in (7), and discuss the significance of the

particular values selected. We also make some observations on the practical implementation of our chosen error estimates.

Perhaps the most fundamental parameter in our anisotropic algorithm is the maximum permitted aspect ratio, which is taken to be 256 for the examples in Section 3. One advantage of this choice is that, for the sizes of mesh that we consider, the maximum AR is reached before the end of the refinement process and so we are able to observe that the rate of convergence reverts back to approximately one for further refinements. From a theoretical point of view however there is a strong argument against imposing any such upper limit. Instead one could just rely on the refinement selection mechanism (5) to decide whether anisotropic refinement is no longer appropriate since, for any fixed choice of κ, this situation should eventually arise. Practically however this approach leads to a number of difficulties (although, if these can be overcome, permitting larger aspect ratios certainly can deliver superior results in terms of the energy norm of the error versus the number of unknowns).

A major problem, for example, is that as the aspect ratios within a finite element mesh grow, the resulting discrete algebraic equations become much more ill-conditioned (even for a fixed number of unknowns). In our linear solver we use the conjugate gradient algorithm with a simple algebraic preconditioner. For maximum efficiency however a hierarchical preconditioner or solver, such as multigrid, should be used. Only if an appropriate algebraic equation solver is applied is it possible to obtain a computational advantage from the fewer degrees of freedom present in an anisotropic mesh. This issue of the use of hierarchical solvers on anisotropic grids is discussed in further detail in [4, Section 6.3] for example.

Another difficulty with using extremely anisotropic elements arises in the solution of the approximate error equations used to obtain the AB and AO estimates. These estimates require the solution of a Neumann boundary value problem on each element, which is usually undertaken with the aid of a small finite element calculation (e.g. using nine or ten cubic basis functions or ten piecewise linear basis functions: we have implemented both but use the latter in this work). Unfortunately, as the aspect ratio of an element grows these systems get harder to solve numerically. Indeed, once the AR reaches about 10^4, it is very difficult to obtain any solution at all since the finite element system becomes singular in floating point arithmetic (despite the fact that, analytically, it is always non-singular for $\kappa > 0$).

A further significant parameter is our choice of $C = \frac{1}{2}$ in (7). Recall that unless (7) is satisfied, anisotropic refinement is not permitted and so increasing C allows such refinement to occur for a larger relative component of the L^2 norm of the error. It is apparent from the first graph in Figure 3 that in some cases $C = \frac{1}{2}$ is too cautious a choice (since the ZZ estimate performs better than using the exact error, due to the fact that the former has no L^2 component). Our initial implementation of the adaptive algorithm uses $C = 1$ however this generally performs poorly on our second example (and problems similar to it). Less extreme choices for the value of C tend to yield similar performance to $C = \frac{1}{2}$: altering the point at which the anisotropic refinement begins but generally leading to final meshes of a very similar quality.

The choice of the exact interval on the right-hand side of (5) is also not too critical.

Clearly when the quotient on the left-hand side is either very large or very small then we would wish to refine anisotropically (provided that (7) is satisfied). Similarly, when the quotient is very near to one, uniform refinement is appropriate. Calculations using the intervals $[\frac{1}{3}, 3]$ and $[\frac{3}{4}, \frac{4}{3}]$ for example both lead to results for which the graphs of error against unknowns are virtually identical to those obtained when using the interval $[\frac{1}{2}, 2]$ in (5).

Our final remarks concerning implementation issues relate to the complexity of the implementation and the cost of execution of each of the error estimates that have been considered. For the exact error calculations on each triangle we have used a 7-point quadrature rule with algebraic degree of precision 5 throughout this work. A small number of calculations with a more accurate formula (37 points and degree of precision 13) show that the 7-point formula is adequate in almost all cases. The only inaccuracies occur on very coarse grids but these tend to be refined in an identical manner whichever formula is used. Other than the numerical calculation of the energy norm of the exact error, the simplest estimate to compute is ZZ since, unlike the other estimates that we have considered, this does not require any error equations to be solved. The most complex estimate to implement and compute is AB (closely followed by AO) as this requires the careful calculation of Neumann data for the error equations on each triangular element. The BW estimate also requires an error equation to be solved on each triangle however the edge data is far simpler to compute and it is only necessary to solve a 3×3 linear system on each element.

5 Discussion

The numerical calculations reported in Sections 2 and 3 are all based upon $\kappa = 10^3$, which is chosen to be representative of large values of κ. When much smaller values of κ are used the anisotropy in the problem decreases and there is less to choose between the different error estimates in terms of the refinements that they induce. In the limiting case where $\kappa = 0$ the solutions to our test problems are simple smooth functions. However, choosing the right-hand side of (1) appropriately it is possible to manufacture an artificial problem whose solution contains a steep boundary or internal layer. In this situation the energy norm reduces to the H^1 semi-norm and the resulting problem has been considered by a number of authors, including [15, 18, 23]. Our approach works well in this case too however, in practice one would always choose an initial mesh that is able to approximate the data, f in (1), accurately (see, for example, [15, 21]). Hence the initial mesh for this type of problem should always be anisotropic when an anisotropic refinement algorithm is available. There are situations in three dimensions however where an anisotropic solution exists to the Poisson problem with an isotropic right-hand side on certain domains: see [4, 18] for example.

There are a number of additional computational comparisons that could be made in order to obtain further data on the performance of our proposed technique. One particular approach would be to produce a hybrid algorithm based upon combining ZZ with an estimate which is able to provide an approximation to the L^2 norm of the error. This

could be achieved in at least two ways. For example, the AB estimate, say, could be used until (7) is satisfied and then the ZZ estimate could be used instead. Alternatively, the two estimates could be combined so as to estimate the energy norm of the error by the sum of the L^2 norm of the AB estimate plus the ZZ estimate. Initial experiments with the first of these strategies are very encouraging: generally leading to an improvement over the use of AB alone.

Further comparisons, against existing *ad hoc* refinement strategies, such as [3, 14, 23], would also be worth undertaking. The difficulty with this however is that most such strategies implicitly link the criteria for adapting the mesh with the process used for executing the adaptivity. This link makes reliable comparisons quite difficult to achieve. A Hessian approach (e.g. [14]) might be used within the context of our existing refinement algorithm however by only performing anisotropic refinement when eigenvectors of the Hessian are nearly parallel with rectangle edges.

One of the main advantages of the simple mesh refinement algorithm used in this work is its lack of complexity. This therefore allows us concentrate on assessing the quality of the information that we are able to extract from the exact error and the selected error estimates. For practical problems however this Cartesian refinement algorithm is not sufficiently general since there is a need to be able to align an anisotropic mesh with solution features which may occur in arbitrary directions. It is not the goal of this short paper to consider algorithms for undertaking refinement in this general manner, however we do expect the ideas introduced here still to be applicable in such cases. In particular, provided the adaptivity procedure is able to produce an anisotropic mesh that is well aligned with the anisotropy present in the solution (see, for example, [18] for a discussion of a matching function which is able to quantify this), then it should be possible to drive this adaptivity using the approach described in this work. Developing such an adaptive algorithm, which should be robust and, ideally, maintain the hierarchical data structures required for the fast solution of very poorly conditioned systems of equations, is still a topic of current research however.

Acknowledgements

We are grateful to Gerd Kunert for the valuable discussions that we have had with him whilst undertaking this work which was supported by the DAAD and British Council under the ARC programme. The work of SG was supported by a grant from the state of Saxony, FRG.

References

[1] M. Ainsworth and I. Babuška. Reliable and robust a posteriori error estimation for singularly perturbed reaction–diffusion problems. *SIAM J. Num. Anal.*, 36(2):331–353, 1999.

[2] M. Ainsworth and J.T. Oden. A posteriori error estimation in finite element analysis. *Comput. Methods Appl. Mech. Eng.*, 142(1-2):1–88, 1997.

[3] D. Ait-Ali-Yahia, W.G. Habashi, A. Tam, M.-G. Vallet, and M. Fortin. A directionally adaptive methodology using an edge-based error estimate on quadrilateral grids. *Int. J. Numer. Methods Fluids*, 23:673–690, 1996.

[4] Th. Apel. *Anisotropic finite elements: Local estimates and applications.* Advances in Numerical Mathematics. Teubner, Stuttgart, 1999. Habilitationsschrift.

[5] Th. Apel and F. Milde. Comparison of several mesh refinement strategies near edges. *Comm. Numer. Methods Engrg.*, 12:373–381, 1996.

[6] Th. Apel, R. Mücke, and J. R. Whiteman. Incorporation of a-priori mesh grading into a-posteriori adaptive mesh refinement. In A. Casal, L. Gavete, C. Conde, and J. Herranz, editors, *III Congreso Matemática Aplicada/XIII C.E.D.Y.A. Madrid, 1993*, pages 79–92, Madrid, 1995. Shortened version of Report 93/9, BICOM Institute of Computational Mathematics, 1993.

[7] R.E. Bank and A. Weiser. Some a posteriori error estimates for elliptic partial differential. *Math. Comp.*, 44:283–301, 1985.

[8] R. Beinert and D. Kröner. Finite volume methods with local mesh alignment in 2–D. In *Adaptive Methods – Algorithms, Theory and Applications*, volume 46 of *Notes on Numerical Fluid Mechanics*, pages 38–53, Braunschweig, 1994. Vieweg.

[9] J.U. Brackbill. An adaptive grid with directional control. *J. Comp. Phys.*, 108:38–50, 1993.

[10] G.C. Buscaglia and E.A. Dari. Anisotropic mesh optimization and its application in adaptivity. *Int. J. Numer. Methods Eng.*, 40(22):4119–4136, 1997.

[11] M. J. Castro-Díaz, F. Hecht, and B. Mohammadi. New progress in anisotropic grid adaption for inviscid and viscous flow simulations. In *Proceedings of the* 4^{th} *Annual International Meshing Roundtable*, pages 73–85, Albuquerque, NM, 1995. Sandia National Laboratories. Also Report 2671 at INRIA.

[12] E. F. D'Azevedo and R. B. Simpson. On optimal triangular meshes for minimizing the gradient error. *Numer. Math.*, 59:321–348, 1991.

[13] M. Dobrowolski, S. Gräf, and C. Pflaum. On a posteriori error estimators in the finite element method on anisotropic meshes. *Electronic Transactions Num. Anal.*, 8:36–45, 1999.

[14] V. Dolejší. Anisotropic mesh adaptation for finite volume and finite element methods on triangular meshes. *Comput. Vis. Sci.*, 1(3):165–178, 1998.

[15] W. Dörfler. A convergent adaptive algorithm for poisson's equation. *SIAM J. Numer. Anal.*, 33:1106–1124, 1996.

[16] T. Iliescu. A 3D flow-aligning algorithm for convection-diffusion problems. *App. Math. Letters*, 12(4):67–70, 1999.

[17] R. Kornhuber and R. Roitzsch. On adaptive grid refinement in the presence of internal and boundary layers. *IMPACT of Computing in Sci. and Engrg.*, 2:40–72, 1990.

[18] G. Kunert. *A posteriori error estimation for anisotropic tetrahedral and triangular finite element meshes.* PhD thesis, TU Chemnitz, 1999. Logos, Berlin, 1999.

[19] G. Kunert. Robust local problem error estimation for a singularly perturbed problem on anisotropic finite element meshes. Preprint SFB393/01-01, TU Chemnitz, 2001.

[20] N. Madden and M. Stynes. Efficient generation of oriented meshes for solving convection-diffusion problems. *Int. J. Num. Meth. Eng.*, 40:565–576, 1997.

[21] P. Morin, R. H. Nochetto, and K. Siebert. Data oscillation and convergence of adaptive FEM. Preprint 17/1999, Albert-Ludwigs-Universität Freiburg, Mathematische Fakulät, 1999.

[22] J. Peraire, M. Vahdati, K. Morgan, and O. C. Zienkiewicz. Adaptive remeshing for compressible flow computation. *J. Comp. Phys.*, 72:449–466, 1987.

[23] W. Rachowicz. An anisotropic h-type mesh refinement strategy. *Comput. Methods Appl. Mech. Engrg.*, 109:169–181, 1993.

[24] W. Rick, H. Greza, and W. Koschel. FCT-solution on adapted unstructured meshes for compressible high speed flow computations. In E. H. Hirschel, editor, *Flow simulation with high-performance computers I*, volume 38 of *Notes on Num. Fluid Mechanics*, pages 334–438. Vieweg, 1993.

[25] K. G. Siebert. An a posteriori error estimator for anisotropic refinement. *Numer. Math.*, 73(3):373–398, 1996.

[26] R. B. Simpson. Anisotropic mesh transformation and optimal error control. *Appl. Numer. Math.*, 14:183–198, 1994.

[27] T. Skalický and H.-G. Roos. Anisotropic mesh refinement for problems with internal and boundary layers. *Int. J. Numer. Methods Eng.*, 46:1933–1953, 1999.

[28] O. C. Zienkiewicz and J. Wu. Automatic directional refinement in adaptive analysis of compressible flows. *Internat. J. Numer. Methods Engrg.*, 37:2189–2210, 1994.

[29] O. C. Zienkiewicz and J. Z. Zhu. A simple error estimator and adaptive procedure for practical engineering analysis. *Internat. J. Numer. Methods Engrg.*, 24:337–357, 1987.

Other titles in the SFB393 series:

00-01 G. Kunert. Anisotropic mesh construction and error estimation in the finite element method. January 2000.

00-02 V. Mehrmann, D. Watkins. Structure-preserving methods for computing eigenpairs of large sparse skew-Hamiltonian/Hamiltonian pencils. January 2000.

00-03 X. W. Guan, U. Grimm, R. A. Römer, M. Schreiber. Integrable impurities for an open fermion chain. January 2000.

00-04 R. A. Römer, M. Schreiber, T. Vojta. Disorder and two-particle interaction in low-dimensional quantum systems. January 2000.

00-05 P. Benner, R. Byers, V. Mehrmann, H. Xu. A unified deflating subspace approach for classes of polynomial and rational matrix equations. January 2000.

00-06 M. Jung, S. Nicaise, J. Tabka. Some multilevel methods on graded meshes. February 2000.

00-07 H. Harbrecht, F. Paiva, C. Perez, R. Schneider. Multiscale Preconditioning for the Coupling of FEM-BEM. February 2000.

00-08 P. Kunkel, V. Mehrmann. Analysis of over- and underdetermined nonlinear differential-algebraic systems with application to nonlinear control problems. February 2000.

00-09 U.-J. Görke, A. Bucher, R. Kreißig, D. Michael. Ein Beitrag zur Lösung von Anfangs-Randwert-Problemen einschließlich der Materialmodellierung bei finiten elastisch-plastischen Verzerrungen mit Hilfe der FEM. März 2000.

00-10 M. J. Martins, X.-W. Guan. Integrability of the D_n^2 vertex models with open boundary. March 2000.

00-11 T. Apel, S. Nicaise, J. Schöberl. A non-conforming finite element method with anisotropic mesh grading for the Stokes problem in domains with edges. March 2000.

00-12 B. Lins, P. Meade, C. Mehl, L. Rodman. Normal Matrices and Polar Decompositions in Indefinite Inner Products. March 2000.

00-13 C. Bourgeois. Two boundary element methods for the clamped plate. March 2000.

00-14 C. Bourgeois, R. Schneider. Biorthogonal wavelets for the direct integral formulation of the heat equation. March 2000.

00-15 A. Rathsfeld, R. Schneider. On a quadrature algorithm for the piecewise linear collocation applied to boundary integral equations. March 2000.

00-16 S. Meinel. Untersuchungen zu Druckiterationsverfahren für dichteveränderliche Strömungen mit niedriger Machzahl. März 2000.

00-17 M. Konstantinov, V. Mehrmann, P. Petkov. On Fractional Exponents in Perturbed Matrix Spectra of Defective Matrices. April 2000.

00-18 J. Xue. On the blockwise perturbation of nearly uncoupled Markov chains. April 2000.

00-19 N. Arada, J.-P. Raymond, F. Tröltzsch. On an Augmented Lagrangian SQP Method for a Class of Optimal Control Problems in Banach Spaces. April 2000.

00-20 H. Harbrecht, R. Schneider. Wavelet Galerkin Schemes for 2D-BEM. April 2000.

00-21 V. Uski, B. Mehlig, R. A. Römer, M. Schreiber. An exact-diagonalization study of rare events in disordered conductors. April 2000.

00-22 V. Uski, B. Mehlig, R. A. Römer, M. Schreiber. Numerical study of eigenvector statistics for random banded matrices. May 2000.

00-23 R. A. Römer, M. Raikh. Aharonov-Bohm oscillations in the exciton luminescence from a semiconductor nanoring. May 2000.

00-24 R. A. Römer, P. Ziesche. Hellmann-Feynman theorem and fluctuation-correlation analysis of i the Calogero-Sutherland model. May 2000.

00-25 S. Beuchler. A preconditioner for solving the inner problem of the p-version of the FEM. May 2000.

00-26 C. Villagonzalo, R.A. Römer, M. Schreiber, A. MacKinnon. Behavior of the thermopower in amorphous materials at the metal-insulator transition. June 2000.

00-27 C. Mehl, V. Mehrmann, H. Xu. Canonical forms for doubly structured matrices and pencils. June 2000. S. I. Solov'ev. Preconditioned gradient iterative methods for nonlinear eigenvalue problems. June 2000.

00-29 A. Eilmes, R. A. Römer, M. Schreiber. Exponents of the localization lengths in the bipartite Anderson model with off-diagonal disorder. June 2000.

00-30 T. Grund, A. Rösch. Optimal control of a linear elliptic equation with a supremum-norm functional. July 2000.

00-31 M. Bollhöfer. A Robust ILU Based on Monitoring the Growth of the Inverse Factors. July 2000.

00-32 N. Arada, E. Casas, F. Tröltzsch. Error estimates for a semilinear elliptic control problem. July 2000.

00-33 T. Penzl. LYAPACK Users Guide. August 2000.

00-34 B. Heinrich, K. Pietsch. Nitsche type mortaring for some elliptic problem with corner singularities. September 2000.

00-35 P. Benner, R. Byers, H. Faßbender, V. Mehrmann, D. Watkins. Cholesky-like Factorizations of Skew-Symmetric Matrices. September 2000.

00-36 C. Villagonzalo, R. A. Römer, M. Schreiber, A. MacKinnon. Critical Behavior of the Thermoelectric Transport Properties in Amorphous Systems near the Metal-Insulator Transition. September 2000.

00-37 F. Milde, R. A. Römer, M. Schreiber. Metal-insulator transition in anisotropic systems. October 2000.

00-38 T. Stykel. Generalized Lyapunov Equations for Descriptor Systems: Stability and Inertia Theorems. October 2000.

00-39 G. Kunert. Robust a posteriori error estimation for a singularly perturbed reaction-diffusion equation on anisotropic tetrahedral meshes. November 2000.

01-01 G. Kunert. Robust local problem error estimation for a singularly perturbed problem on anisotropic finite element meshes. January 2001.

01-02 G. Kunert. A note on the energy norm for a singularly perturbed model problem. January 2001.

01-03 U.-J. Görke, A. Bucher, R. Kreißig. Ein Beitrag zur Materialparameteridentifikation bei finiten elastisch-plastischen Verzerrungen durch Analyse inhomogener Verschiebungsfelder mit Hilfe der FEM. Februar 2001.

01-04 R. A. Römer. Percolation, Renormalization and the Quantum-Hall Transition. February 2001.

01-05 A. Eilmes, R. A. Römer, C. Schuster, M. Schreiber. Two and more interacting particles at a metal-insulator transition. February 2001.

01-06 D. Michael. Kontinuumstheoretische Grundlagen und algorithmische Behandlung von ausgewählten Problemen der assoziierten Fließtheorie. März 2001.

01-07 S. Beuchler. A preconditioner for solving the inner problem of the p-version of the FEM, Part II - algebraic multi-grid proof. March 2001.

01-08 S. Beuchler, A. Meyer. SPC-PM3AdH v 1.0 - Programmer's Manual. March 2001.

01-09 D. Michael, M. Springmann. Zur numerischen Simulation des Versagens duktiler metallischer Werkstoffe (Algorithmische Behandlung und Vergleichsrechnungen). März 2001.

01-10 B. Heinrich, S. Nicaise. Nitsche mortar finite element method for transmission problems with singularities. March 2001.

01-11 T. Apel, S. Grosman, P. K. Jimack, A. Meyer. A New Methodology for Anisotropic Mesh Refinement Based Upon Error Gradients. March 2001.

The complete list of current and former preprints is available via
`http://www.tu-chemnitz.de/sfb393/preprints.html`.